Strain-induced magnetism in ReS_2 monolayer with defects*

Xiao-Ou Zhang(张小欧)[1] and Qing-Fang Li(李庆芳)[2,†]

[1] *Department of Electrical Engineering and Photoelectric Technology, Zijin College of Nanjing University of Science and Technology, Nanjing* 210023, *China*
[2] *Department of Physics, Nanjing University of Information Science & Technology, Nanjing* 210044, *China*

(Received 21 April 2016; revised manuscript received 2 June 2016; published online 30 September 2016)

We investigate the effects of strain on the electronic and magnetic properties of ReS_2 monolayer with sulfur vacancies using density functional theory. Unstrained ReS_2 monolayer with monosulfur vacancy (V_S) and disulfur vacancy (V_{2S}) both are nonmagnetic. However, as strain increases to 8%, V_S-doped ReS_2 monolayer appears a magnetic half-metal behavior with zero total magnetic moment. In particular, for V_{2S}-doped ReS_2 monolayer, the system becomes a magnetic semiconductor under 6% strain, in which Re atoms at vicinity of vacancy couple anti-ferromagnetically with each other, and continues to show a ferromagnetic metal characteristic with total magnetic moment of 1.60μ_B under 7% strain. Our results imply that the strain-manipulated ReS_2 monolayer with V_S and V_{2S} can be a possible candidate for new spintronic applications.

Keywords: ReS_2, first-principle calculations, strain, defect

PACS: 71.15.Mb, 73.20.At, 75.50.Pp **DOI:** 10.1088/1674-1056/25/11/117103

1. Introduction

Due to unique electronic properties and chemical stability, tremendous research efforts have been focused on layered transition-metal dichalcogenides (TMDCs) considered as promising potential candidates on electronic, optoelectronic, and photovoltaic applications.[1–8] As a popular member of TMDCs, MoS_2 monolayer is a two-dimensional (2D) material with bandgap suitable for logic device application,[9–11] and can be easily synthesized through chemical growth.[12,13] Unfortunately, when increased the number of layers and applied small strain, MoS_2 undergoes a crossover from direct to indirect band gap, which poses great challenge in making robust optoelectronic devices based on MoS_2.[14,15] Recently, as a new member of TMDCs, ReS_2 monolayer was experimentally produced through chemical exfoliation process and attracted a lot of attentions.[16–24] The vanishing interlayer coupling in ReS_2 make its direct band gap (1.55 eV) no dependence on the number of layers. Such insensitivity of band gap on layers enables fabrication of 2D optoelectronic devices without the need for monolayers.[16]

For prospective applications in low-dimensional spintronic devices, considerable efforts have been devoted to explore the magnetic behavior of TMDCs. It is well known that adding the spin degree of freedom to conventional semiconductor charge-based electronics will add substantially more capability and performance to electronic products, and the operation of spintronic devices require generation and detection of tunable spin currents, which can ideally be done using a ferromagnetic semiconductor.[25–28] However, pristine (P-) ReS_2 monolayer is intrinsically nonmagnetic. So developing approaches to effectively induce and manipulate the magnetism are crucial for facilitating application of monolayer ReS_2 on low-dimensional spintronic devices. It is well known that vacancy defects in chemically grown 2D materials are noticeable due to the imperfection of the growth process, and can be controllably achieved by chemical vapor deposition, field evaporation, and electron irradiation methods.[29,30] These structural defects can have a significant influence on the magnetic properties of 2D materials. Recently, Horzum *et al.* found that some commonly observed vacancies in ReS_2 monolayer, sulfur defects, do not result in any spin polarization, while Re-containing defects induce magnetization with a net magnetic moment of 1–3 μ_B.[21]

Strain has been known as an effective mechanism for controlling magnetic properties of 2D materials, which can sustain larger strains than bulk crystals. For example, MoS_2 monolayer and graphene have been reported to be strained up to 11% and 15% before rupture.[31–33] Some theoretical reports have proposed that the appropriate tensile train can induce or manipulate the magnetic properties of vacancy-doped MoS_2 monolayers.[34–36] The tensile strain appears to be more effective in modulating the magnetic properties of 2D TMDCs than compressive strain, and Re-containing vacancies in ReS_2 monolayer result in a sizable magnetic moment and have higher formation energy than Sulfur vacancies.[21] Therefore, in this letter we only investigate a possible emergence of magnetism in monosulfur vacancy (V_S) and disulfur vacancy (V_{2S}) doped ReS_2 monolayers under biaxial tensile strain, and explore the physical mechanism about strain induced magnetism in vacancy-doped ReS_2 monolayer.

*Project supported by the National Natural Science Foundation of China (Grant No. 11547030).
†Corresponding author. E-mail: qingfangli@nuist.edu.cn
© 2016 Chinese Physical Society and IOP Publishing Ltd

2. Computational method

Our calculations were performed in the frame work of density functional theory (DFT) as implemented in the Vienna *ab-initio* simulation package (VASP).[37,38] The generalized gradient approximation (GGA) within Perdew–Burke–Ernzerhof (PBE) formalism[39] was employed for exchange-correlation potential. The projector augmented wave (PAW) method[40] and a plane-wave basis set with an energy cut-off of 500 eV were used in the calculations. A 5×5×1 Monkhorst–Pack *k*-mesh was used for an integration over the Brillouin zone. The convergence criterion of self-consistency and atomic Hellman–Feynman forces were set to be 10^{-5} eV and 0.01 eV/Å, respectively. A large vacuum spacing (at least 15 Å) was used to avoid interaction between ReS_2 layers. The defects were obtained by removing the relevant atoms from a 2×2 supercell. The convergence of defect formation energy was checked by varying the size of supercell.

Calculations with a 3×3 supercell show that the formation energies of defects all are converged on the order of only 0.01 eV. The strain ε can be defined as $\varepsilon = (a - a_0)/a_0 \times 100\%$, where a and a_0 is the lattice constants of strain and unstrained system, respectively. Under each biaxial strain, all atoms are fully relaxed with fixed lattice constant.

3. Results and discussion

Due to the distorted 1T structure, there are two and four inequilavent Re and S sites on the ReS_2 monolayer, which are possible for fabricating point defects as shown in Fig. 1(a). We only investigate the relative stability of Sulfur point defects by calculating the formation energy

$$E_f = E_d + n\mu_S - E_p, \quad (1)$$

where E_d and E_p are total energies of ReS_2 supercell with and without defects, respectively. μ_S is the chemical potential of the removed S atom, i.e., the total energy per atom of S orthorhombic crystal.

Due to the distorted lattice structure of ReS_2, the formation of S-vacancies is site dependent. The values presented in Table 1 are the formation energies of those vacancy sites with the lowest formation energy under several strains.

Table 1. Formation energies E_f of V_S and V_{2S} doped ReS_2 monolayers under several strains for the Re-rich and the S-rich cases.

ε	V_S		V_{2S}	
	Re-rich	S-rich	Re-rich	S-rich
0%	1.21	2.08	2.87	4.62
1%	1.36	2.23	3.15	4.90
2%	1.47	2.34	3.36	5.11
3%	1.56	2.43	3.51	5.26
4%	1.62	2.49	3.59	5.34
5%	1.66	2.53	3.61	5.36
6%	1.66	2.53	3.57	5.32
7%	1.64	2.51	3.46	5.21
8%	1.54	2.41	3.06	4.81

The unstrained systems are first investigated. Through our calculation results, we find that Vs, shown in Fig. 1(b), is more easily created with the formation energy of 2.08 eV (S-rich condition) in four different monosulfur vacancies. In the plenty of possibility to create disulfur vacancy, V_{2S} shown in Fig. 1(c) has the lowest formation energy with the value of 4.62 eV (S-rich condition), which is similar with previous calculation result.[21] Our results show that the formation energy of V_{2S} is larger than twice that of V_S, suggesting that single sulfur vacancy have no tendency to combine to form the disulfur vacancy and can be introduced more easily in ReS_2 monolayer. The magnetic energy, which represents the energy gained from the spin polarization, is calculated as $\Delta E_m = E_{NM} - E_{MAG}$ for vacancy-doped ReS_2 monolayer. That the obtained magnetic energy is zero indicates that V_S and V_{2S} do not induce magnetism in unstrained ReS_2 monolayer. The calculated result is consistent with previous report.[21]

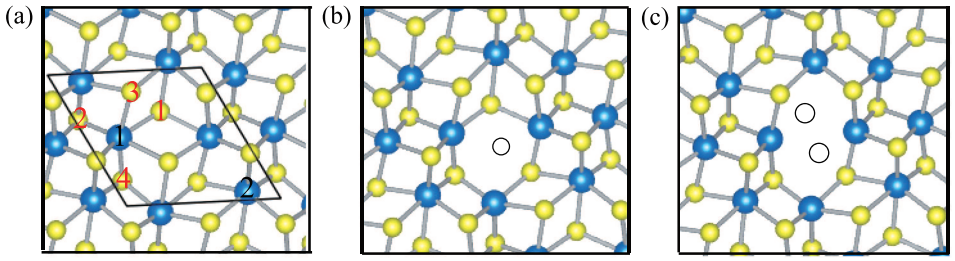


Fig. 1. (color online) The top view of optimized atomic structures of (a) pristine-, (b) V_S-, and (c) V_{2S}-doped ReS_2 monolayers. Missing S atoms are shown by empty gray circles. In panel (a), the numbered atoms with black and red colors indicate the possible inequivalent sites for creating Re and S vacancies, respectively.

Next, the strain from 0% to 8% is applied for vacancy-doped ReS_2 monolayer. V_S doped systems remain nonmagnetic when strain is smaller than 8% and then transform to magnetic state. As displayed from the spin resolved charge density in Fig. 2(a), the distribution of spin density is predominantly located at three Re atoms around vacancy, in which anti-ferromagnetic (AFM) couplings are introduced between the spins of Re1 atom ($0.263\mu_B$), Re2 and Re3 atoms with the magnetic moment of $-0.065\mu_B$ and $-0.188\mu_B$. Furthermore, the other atoms at vicinity of vacancy also exhibit visible spin

polarizations, so that the system exhibits a magnetic behavior with the total magnetic moment of zero. The magnetic energy is only 12 meV, indicating the unstability of the magnetic state at room temperature. The magnetic behavior is different from the formation of a magnetic moment of $2\mu_B$ in V_S-doped MoS_2 monolayer under 9% tensile strain.[35] In strained V_S-doped MoS_2 monolayer, due to the symmetry of MoS_2 monolayer, three Mo atoms at vicinity of vacancy toward to the vacancy spot form an equilateral triangle, and have to be ferromagnetically (FM) coupled each other under consideration of spin frustration. However, due to distorted 1T structure in ReS_2 monolayer, three Re atoms around S-vacancy (Re1, Re2, and Re3) are inequivalent, and the distances between Re1, Re2, Re3 atoms and missing S atom in P-ReS_2 monolayer are 2.47 Å, 2.48 Å, and 2.46 Å, respectively. This condition improves the possibility of AFM coupling behavior in strained V_S-doped ReS_2 monolayer.

For V_{2S}-doped ReS_2 monolayer, the system remains nonmagnetic when strain is smaller than 6%, and then transforms to a magnetic behavior, in which the spin magnetizations are mostly contributed from Re1 and Re2 atoms around vacancy with local moments of $0.308\mu_B$ and $-0.308\mu_B$, shown in Fig. 2(b). When strain continuously increases to 7%, FM behavior with the total magnetic moment of $1.60\mu_B$ appears in system, in which the local moments are mainly contributed by the 5d orbital of Re1 ($0.238\mu_B$), Re2 ($0.238\mu_B$), Re3 ($0.125\mu_B$), Re4 ($0.125\mu_B$), Re5 ($0.093\mu_B$), and Re6 ($0.093\mu_B$) atoms. We find that the spatial extension of spin density under 6% strain is smaller than that under 7% strain. The magnetic energy (21 meV) under 7% strain is larger than that (12 meV) under 6% strain, indicating stronger magnetic stability with increasing strain.

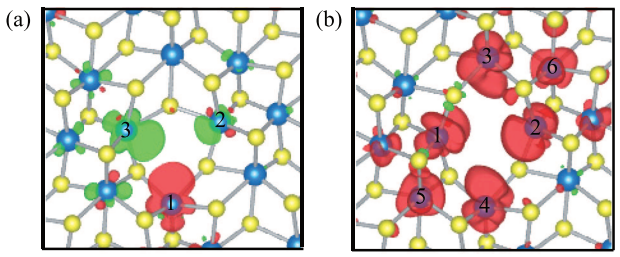


Fig. 2. (color online) The spin resolved charge densities for (a) V_S-doped ReS_2 monolayer under 8% strain and (b) V_{2S}-doped ReS_2 monolayer under 7% strain. The isosurface value is 0.001 e/Å. Red (green) colors represent spin up (down) electrons. The spin polarizations are mainly contributed from the numbered atoms in panels (a) and (b).

To get an insight into the strain-induced magnetism, we study the strain effect on electronic structures and stability. Figure 3 shows the strain dependence of band gap and formation energy in vacancy-doped ReS_2 monolayer. All band gaps decrease with increasing tensile strain. For the P-ReS_2 monolayer, the band gap drops steadily with the strain, only 0.78 eV at 8%, which is similar to linearly dropping in P-MoS_2 monolayer.[34] For V_S- and V_{2S}-doped ReS_2 monolayers, band gaps are smaller than that of P-ReS_2 monolayer and drop to zero at 8% and 7% strains, respectively. It is interesting that under the strain of 6%, there has been a magnetic state (Re atoms at vicinity of vacancy are AFM coupled with each other) when band gap is 0.19 eV in V_{2S}-doped ReS_2 monolayer. This is different from the case for vacancy-doped MoS_2 monolayer, where the critical strain value for band gap closing agrees with that for magnetic state emergence.[34] As shown in Fig. 3(b), the formation energy increase and reach maximum at 5% strain, then drop slightly. Encouragingly, under critical tensile strain of magnetism emergence, the vacancy stability is very close to zero strain, which enables fabrication of magnetic V_S- and V_{2S}-doped ReS_2 monolayers in experiment.

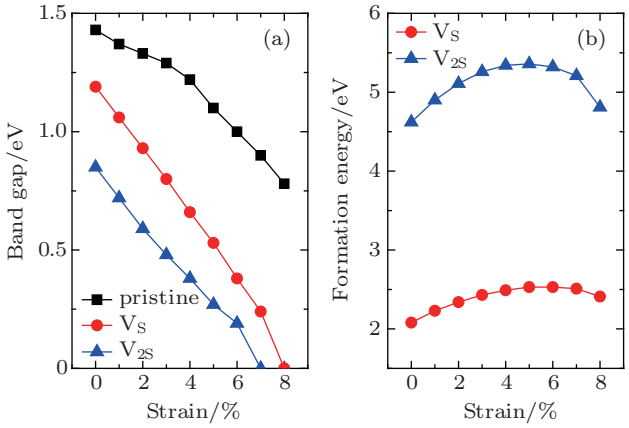


Fig. 3. (color online) (a) Band gap and (b) formation energy as a function of tensile strain.

To explore the physical mechanism of the emergent magnetic behavior of defective ReS_2 monolayer under tensile strain, the total density of states (DOS) and projected DOS are illustrated in Fig. 4. Comparing the DOS of P-ReS_2 monolayer, we find that the formation of V_S produces a defect level locating close to the valence band maximum (VBM), reducing the band gap from 1.43 eV (band gap of P-ReS_2 monolayer) to 1.19 eV, while the formation of V_{2S} produces two defect levels locating at close to the VBM and the conduct band minimum (CBM), dramatically reducing the band gap of P-ReS_2 monolayer to 0.85 eV. All these defect states contribute from 5d orbitals of Re atoms at the vicinity of vacancy. With increasing strain, all the conduct band levels shift downwards and start to interact with the valence band levels around the Fermi level. Under the strain of 8%, V_S-doped system exhibits half-metal behavior, with a band gap of 0.08 eV in majority spin channel and a partially occupied band in minority spin channel. Under the strain of 7%, V_{2S}-doped system is shown to be metallic, i.e., the band gap collapses. The spin majority bands and minority bands split, and magnetism appears.

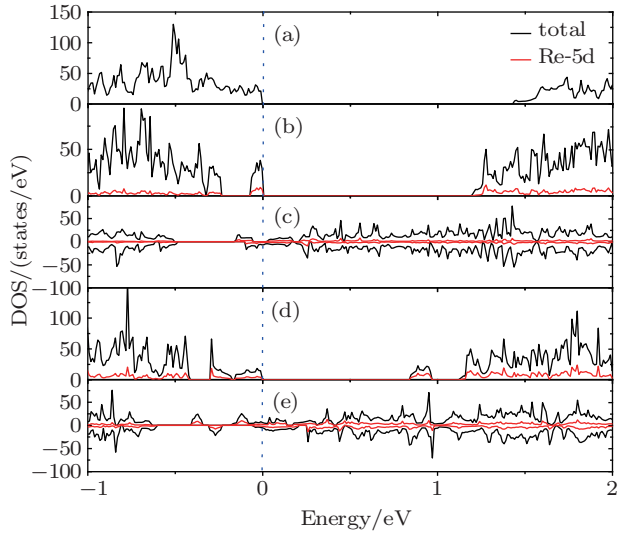


Fig. 4. (color online) Total DOS (black color) of pristine ReS_2 (a), V_S-doped ReS_2 monolayer under 0% (b) and 8% (c) strains, and V_{2S}-doped ReS_2 monolayer under 0% (d) and 7% (e) strains. The corresponding partial DOS (red color) presents the sum of 5d orbitals of nearest Re atoms around the vacancy. Fermi level is denoted by vertical dashed line.

Strain seems indispensable for the magnetism emerging in vacancy-doped ReS_2 monolayer. However, it is important to make sure that magnetism appears before crystal structure breaks. We continue to investigate the V_S- and V_{2S}-doped ReS_2 monolayers in lager strain condition. As shown in Fig. 5, we find that both the structure break under the same strain of 9%, which is slightly beyond the strain for emergence of magnetism. Although the critical strain that makes material breaking in vacancy-doped ReS_2 monolayer is smaller than that in vacancy-doped MoS_2 monolayer,[34] it is still plausible to strain-magnetism in vacancy-doped ReS_2 monolayer in experiment.

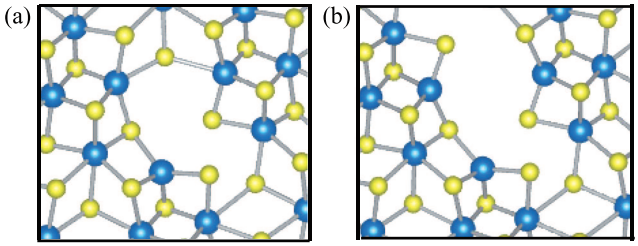


Fig. 5. (color online) (a) V_S- and (b) V_{2S}-doped ReS_2 monolayers under 9% strain.

4. Conclusion

We have systemically explored the strain-induced magnetism in ReS_2 monolayer with V_S and V_{2S}. When the tensile strain of 8% is applied, V_S-doped ReS_2 monolayer results in magnetic half-metal phase, in which Re atoms around vacancy anti-ferromagnetically coupled each other. For V_{2S}-doped ReS_2 monolayer, system has a phase transition from magnetic semiconductor under 6% strain to magnetic metal under 7% strain. Furthermore, the partial extension of spin density in ReS_2 monolayer is increasing with increasing strain. Our results show that strain engineering can provide an effective approach to tune magnetism in vacancy doped ReS_2 monolayer for application on low-dimensional spintronic devices.

References

[1] Castro Neto A H and Novoselov K 2011 *Rep. Prog. Phys.* **74** 082501
[2] Novoselov K S, Jiang D, Schedin F, Booth T J, Khotkevich V V, Morozov S V and Geim A K 2005 *Proc. Natl. Acad. Sci. USA* **102** 10451
[3] Lee C G, Li Q Y, Kalb W, Liu X Z, Berger H, Carpick R W and Hone J 2010 *Science* **328** 76
[4] Radisavljevic B, Radenovic A, Brivio J, Giacometti V and Kis A 2011 *Nat. Nanotechnol.* **6** 147
[5] Cheng F, Ren Y and Sun J F 2015 *Chin. Phys. Lett.* **32** 107301
[6] Guo H H, Yang T, Tao P and Zhang Z D 2014 *Chin. Phys. B* **23** 017201
[7] Xia H D, Li H P, Lan C Y, Li C, Deng G L, Li J F and Liu Y 2015 *Chin. Phys. B* **24** 084206
[8] Zeng L, Xin Z, Chen S W, Du G, Kang J F and Liu X Y 2014 *Chin. Phys. Lett.* **31** 027301
[9] Wang X R, Shi Y and Zhang R 2013 *Chin. Phys. B* **22** 098505
[10] Mak K F, Lee C G, Hone J, Shan J and Heinz T F 2010 *Phys. Rev. Lett.* **105** 136805
[11] Shi H L, Pan H, Zhang Y W and Yakobson B I 2013 *Phys. Rev. B* **87** 155304
[12] Coleman J N, Lotya M, O'Neill A, *et al.* 2011 *Science* **331** 568
[13] Lee Y H, Zhang X Q, Zhang W J, Chang M T, Lin C T, Chang K D, Yu Y C, Wang J T W, Chang C S, Li L J and Lin T W 2012 *Adv. Mater.* **24** 2320
[14] Wang Q H, Kalantar-Zadeh K, Kis A, Coleman J N and Strano M S 2012 *Nat. Nanotechnol.* **7** 699
[15] Ellis J K, Lucero M J and Scuseria G E 2011 *Appl. Phys. Lett.* **99** 261908
[16] Tongay S, Sahin H, Ko C, Luce A, Fan W, Liu K, Zhou J, Huang Y S, Ho C H, Yan J Y, Ogletree D F, Aloni S, Ji J, Li S S, Li J B, Peeters F M and Wu J Q 2014 *Nat. Commun.* **5** 3252
[17] Fujita T, Ito Y, Tan Y W, Yamaguchi H, Hojo D, Hirata A, Voiry D, Chhowalla M and Chen M W 2014 *Nanoscale* **6** 12458
[18] Feng Y Q, Zhou W, Wang Y J, Zhou J, Liu E F, Fu Y J, Ni Z H, Wu X L, Yuan H T, Miao F, Wang B G, Wan X G and Xing D Y 2015 *Phys. Rev. B* **92** 054110
[19] Liu E F, Fu Y J, Wang Y J, *et al.* 2015 *Nat. Commun.* **6** 6991
[20] Zhang E Z, Jin Y B, Yuan X, Wang W Y, Zhang C, Tang L, Liu S S, Zhou P, Hu W D and Xiu F X 2015 *Adv. Funct. Mater.* **25** 4076
[21] Horzum S, Çakir D, Suh J, Tongay S, Huang Y S, Ho C H, Wu J, Sahin H and Peeters F M 2014 *Phys. Rev. B* **89** 155433
[22] Çakir D, Sahin H and Peeters F M 2014 *Phys. Chem. Chem. Phys.* **16** 16771
[23] Yu Z G, Cai Y Q and Zhang Y W 2015 *Sci. Rep.* **5** 13783
[24] Zhang X O and Li Q F 2015 *J. Appl. Phys.* **118** 064306
[25] Wolf S A, Awschalom D D, Buhrman R A, Daughton J M, von Molnár S, Roukes M L, Chtchelkanova A Y and Treger D M 2001 *Science* **294** 1488
[26] Pearton S J, Abernathy C R, Overberg M E, Thaler G T, Norton D P, Theodoropoulou N, Hebard A F, Park Y D, Ren F, Kim J and Boatner L A 2003 *J. Appl. Phys.* **93** 1
[27] MacDonald A H, Schiffer P and Samarth N 2005 *Nat. Mater.* **4** 195
[28] Ohno Y, Young D K, Beschoten B, Matsukura F, Ohno H and Awschalom D D 1999 *Nature* **402** 790
[29] Zhou W, Zou X L, Najmaei S, Liu Z, Shi Y M, Kong J, Lou J, Ajayan P M, Yakobson B I and Idrobo J C 2013 *Nano Lett.* **13** 2615
[30] Komsa H P, Kotakoski J, Kurasch S, Lehtinen O, Kaiser U and Krasheninnikov A V 2012 *Phys. Rev. Lett.* **109** 035503
[31] Lee C G, Wei X D, Kysar J W and Hone J 2008 *Science* **321** 385
[32] Bertolazzi S, Brivio J and Kis A 2011 *ACS Nano* **5** 9703
[33] Cooper R C, Lee C, Marianetti C A, Wei X D, Hone J and Kysar J W 2013 *Phys. Rev. B* **87** 035423
[34] Tao P, Guo H H, Yang T and Zhang Z D 2014 *J. Appl. Phys.* **115** 054305
[35] Zheng H L, Yang B S, Wang D D, Han R L, Du X B and Yan Y 2014 *Appl. Phys. Lett.* **104** 132403
[36] Yun W S and Lee J D 2015 *J. Phys. Chem. C* **119** 2822
[37] Kresse G and Hafner J 1993 *Phys. Rev. B* **47** 558
[38] Kresse G and Furthmüller J 1996 *Phys. Rev. B* **54** 11169
[39] Perdew J P, Burke K and Ernzerhof M 1996 *Phys. Rev. Lett.* **77** 3865
[40] Kresse G and Joubert D 1999 *Phys. Rev. B* **59** 1758